We are IntechOpen, the world's leading publisher of Open Access books Built by scientists, for scientists

4,800
Open access books available

122,000
International authors and editors

135M
Downloads

Our authors are among the

154
Countries delivered to

TOP 1%
most cited scientists

12.2%
Contributors from top 500 universities

CLARIVATE ANALYTICS BOOK CITATION INDEX INDEXED

WEB OF SCIENCE™

Selection of our books indexed in the Book Citation Index in Web of Science™ Core Collection (BKCI)

Interested in publishing with us?
Contact book.department@intechopen.com

Numbers displayed above are based on latest data collected.
For more information visit www.intechopen.com

17

Photoinduced Structural Changes of Doped SiO_2 Glasses using Ultraviolet Laser Pulses

Hiroaki Nishiyama and Junji Nishii
Hokkaido University
Japan

1. Introduction

There is a growing need for photonic band gap (PBG) devices in various applications including high-Q resonators, energy-efficient solar cells, microfluidic devices, microelectromechanical systems and so on. The PBG devices, which have artificial structures whose refractive index is periodically modulated, can reflect or diffract propagating light at a wavelength comparable to lattice spacing. The optical properties of the PBG devices can be controlled by changing lattice patterns, refractive index of lattices, duty ratio, interaction length and so on. Because of high potential for applications, the PBG effects have been intensively studied in the last decade. However, the fabrication of their fine structures, which can work at optical communication wavelengths and visible wavelengths, remains a challenging task.

Most PBG devices are manufactured by the semiconductor fabrication technology including lithography and various etching techniques. Although this technology enables us to create precise structures with high spatial resolution, we must use complicated experimental equipments such as vacuum systems and clean-room environments. In particular, highly expensive electron beam lithography systems are necessary to obtain sub-wavelength photonic structures, which are important for practical applications.

Direct laser writing technique of photonic structures is an attractive alternative. When optical materials are exposed to laser light below ablation threshold intensity, photochemical reactions such as chemical bond breakage and creation or annihilation of lattice defects occur in the laser irradiated regions, , thereby changing the refractive index and density. In 1978, Hill *et al*. firstly reported the direct laser writing of Bragg mirrors (one dimensional PBG devices) inside a Ge-doped SiO_2 core optical fiber using Ar laser (Hill *et al*., 1978). This writing technique enables creation of photonic band gap devices with a simple setup on or in various glasses with sub-wavelength resolution (Svalgraad et al., 1994). Moreover, no debris or cracks are generated, although they often occur with laser ablation or mechanical machining. Especially, pulse laser, which has high peak intensity, is effective for such structural changes. From the point of view of practical applications, the structural changes of SiO_2-based glass materials, which are used as optical fiber or waveguide cores, are more important. Therefore, so far, many researchers have reported the structural changes of glass materials using ultraviolet nanosecond lasers, near-infrared femtosecond laser and so on (Åslund, et al., 2000, Hirao, *et al*., 1997).

Recently, we have reported that crystalline Ge nanoparticles can be patterned in GeO_2-B_2O_3-SiO_2 glass, which is often used as optical fiber or waveguide cores, by a combined process of ultraviolet nanosecond pulse laser irradiation and thermal annealing (Nishiyama, *et al.*, 2004). In general, the laser-induced changes of refractive index are reported to be small and thermally less stable. For example, the refractive index changes induced by ultraviolet laser exposure in optical fiber cores are as small as 10^{-4}, even though photosensitizing processes are used. Furthermore, the index changes start to decay by annealing at 150°C (Baker, *et al.*, 1997). Our combined process is effective for creation of much larger refractive index change with high thermal stability.
In this chapter, we present the fundamentals of pulse laser-induced structural changes of SiO_2-based glasses and the PBG device fabrication using the ultraviolet laser-induced precipitation of Ge nanoparticles in GeO_2-B_2O_3-SiO_2 glass.

2. Fundamentals of laser-induced structural changes

Many reports have described the mechanism of the laser-induced refractive index changes since the first report of Hill's group. However, the details of photochemical reactions related to point defects remain unclear. In this section, we present popular three mechanisms on the refractive index changes. These mechanisms are generally accepted in the field of the direct laser writing of glasses. However, discussion continues about the contribution ratio of each mechanism to the refractive index changes.

2.1 Color center model

GeO_2-SiO_2 glasses often have intense absorption bands around 240 nm in wavelength, which originated from Ge related oxygen deficient defects with relative high stability at high temperature of glass preparation process. When the glass is exposed to laser pulse operating ultraviolet region such as KrF excimer laser of 248 nm wavelength, the intensity of the absorption band bleaches and some other absorption bands appear. This spectral change means that point defects are induced and annihilated in the glass via electronic transitions by the laser irradiation. Hand *et al.* and Dong *et al.* proposed these absorption spectral changes are responsible for the refractive index changes thorough Kramers-Kronig relation (Hand, 1990, Dong, 1995). In fact, highly Ge-doped SiO_2 glasses exhibit larger index changes. Figure 1 shows schematic structures of some defects related to laser-induced refractive index changes.

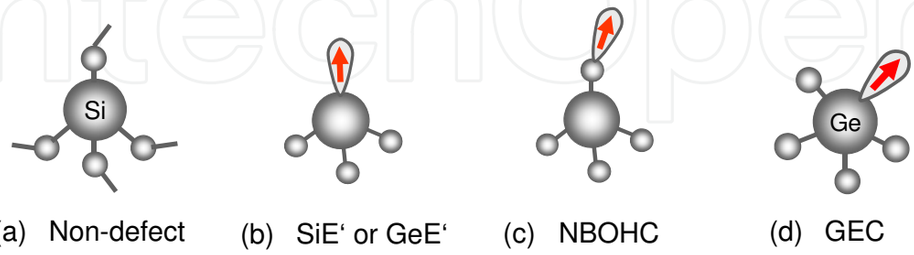

Fig. 1. Color centers in glasses.

2.2 Stress relaxation model

The stress relaxation model is based on the hypothesis that the refractive index changes originate from residual stress in optical fibers through the stress-optic effect (Dong, *et al.*,

2003). Such residual stress are generated mainly from a superposition of thermal stress caused by a difference in thermal expansion coefficients between core and cladding and mechanical stress induced by fiber drawing processes. The ultraviolet laser irradiation can promote the structural relaxation of point defects by ion rearrangements and thermal effect, resulting in refractive index changes of the glasses. In fact, there are several reports on formation of periodic structures using CO_2 laser irradiation and arc discharge as a heat source (Kim, *et al.*, 2001).

2.3 Densification model

Refractive index of glasses is affected by densification changes through Lorentz-Lorenz relation. One of the origins of the density changes is thermal relaxation by laser irradiation. Several groups reported the correlation between the refractive index changes and the densifications of fiber preforms and fibers by the irradiation (Poumellec, et al., 1996, Douay, et al., 1997, Kherbouche, et al., and Fonjallaz et al., 1995). They concluded that the densification mainly contributes to the refractive index changes by theoretical calculation and experimental results. Cordier *et al.* also showed direct evidence of the glass densifications from transmission electron microscope observations of laser irradiated glasses (Cordier *et al.*, 1994). On the other hand, other group reported results that the densification contribution to the refractive index changes is negligible by comparison of measurements and finite-element model calculation (Borrelli, *et al.*, 1999).

3. Direct laser writing methods

To obtain high Q resonance in PBG devices, precise microfabrication of the periodic structures is important. Therefore, to date, several interference techniques have been proposed. In this section, we describe two popular fabrication techniques of PBG devices with sub-wavelength periods using the direct laser writing.

3.1 Two-beam Interference technique

Meltz *et al.* firstly demonstrated the external laser writing of the periodic refractive index modulation on/ in optical fiber cores, which can work as a PBG device, using interference techniques (Meltz *et al.*, 1989). The ultraviolet laser light is split to two beams and later recombined after propagation through different optical paths. This setup enables the formation of sub-wavelength fringe patterns without stitch errors. The grating period Λ can be determined by

$$\Lambda = \lambda / 2\sin\theta \tag{1}$$

where λ and θ are laser wavelength for direct laser writing and half-angle between the intersection beams (see Figure 2(a)). And PBG wavelength (Bragg wavelength) λ_B is given by $\lambda_B = 2N\Lambda$, where N is effective refractive index of fiber core. The advantage of this technique is that it is possible to various Bragg wavelengths by adjusting the interference angles and to obtain large periodic patterns without laser scanning. The long interaction region offers the fabrication of narrow band-pass filters. Furthermore, chirped gratings and curved patterns are also available by changing exposure geometry.

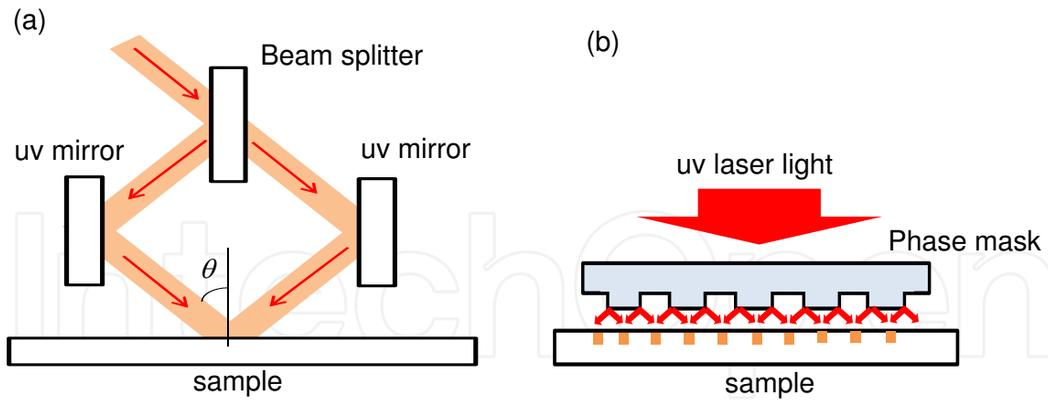

Fig. 2. Schematic depiction of techniques: (a) two-beam interference and (b) the phase mask.

3.2 Phase mask technique

The phase mask technique is one of the most popular writing processes for fine periodic structures. In this technique, diffractive optical elements, called phase masks, are used to modulate incident ultraviolet laser light (Hill, *et al.*, 1993). The phase mask has a one dimensional surface relief on a SiO_2 substrate. When the ultraviolet laser light is normally coupled to the phase mask, the first order diffracted beams are generated from the mask. The zero-order beam is designed to be suppressed to few percentages of the incident power. The samples such as optical fibers or waveguides are located just behind the phase mask. Typically, the distance between the samples and the phase mask is less than 100 μm. In this thin region, a near-field fringe pattern is generated by the interference of the plus and minus first order diffracted beams. The period of this fringe is identical to one-half that of the phase mask. To focus the fringe pattern into the fibers or waveguides, a cylindrical lens is often used. The optical setup of the phase mask technique is simple, compared to the two-beam interference technique. Therefore, it is effective for reproduction of the periodic patterns. KrF excimer laser is one of the popular light sources for the direct laser writing technique. The spatial and temporal coherence of this laser is low. However, low temporal coherence does not affect the writing capability of the phase mask technique.

4. Pulsed laser-induced precipitation of nanoparticles in glasses

4.1 Thermal stabilization of laser-induced refractive index changes

As mentioned in the section 1, the laser-induced structural changes are thermally unstable. Ultraviolet laser pulses can excite electrons of some defect species in glasses and release them. Such released electrons are then trapped in other defects. The structural changes are triggered by these electron excitations. However, thermal energy during annealing excites the trapped electrons again to return back to the original states (Erdogan, *et al.*, 1994). This thermal decay is unavoidable for the laser-induced structural changes in principle. In this section, we present a novel process for the formation of large refractive index changes with excellent thermal stabilities using ultraviolet laser pulses.

Figure 3 shows the changes of the first order diffraction efficiencies of laser-induced gratings (one-dimensional PGB devices) after isochronal annealing for 1 hour at each temperature in a nitrogen atmosphere. The laser-induced grating was written on GeO_2-SiO_2 and

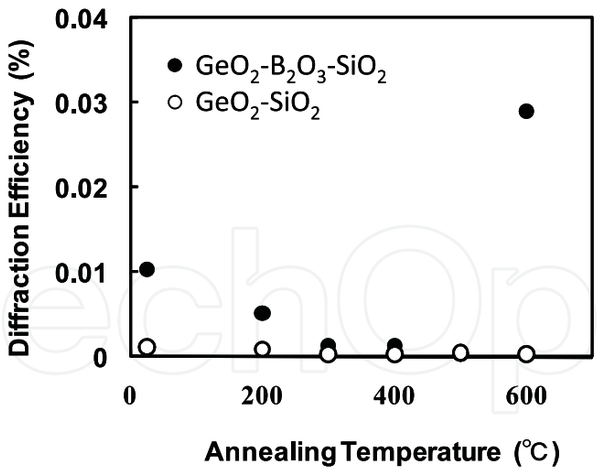

Fig. 3. Changes of diffraction efficiencies of laser-induced gratings after annealing up to 600°C.

GeO_2-B_2O_3-SiO_2 glass thin films using KrF excimer laser (λ = 248 nm) through phase mask of 1060 nm pitch. The glass films were prepared by the plasma-enhanced chemical vapor deposition method using $Si(OC_2H_5)_4$, $Ge(OCH_3)_4$ and $B(OC_2H_5)_3$ as raw materials. The diffraction efficiencies (ratio of diffracted power to incident power) were measured at a probe wavelength of 633 nm under phase matching condition. The diffraction efficiencies for GeO_2-SiO_2 and GeO_2-B_2O_3-SiO_2 decreased gradually after the annealing at a temperature up to 500°C, which was consistent with the previous reports. However, drastic increase of the efficiency for GeO_2-B_2O_3-SiO_2 was observed after annealing at 600°C. Such a drastic change is extremely exceptional phenomenon. This thermally-induced grating in GeO_2-B_2O_3-SiO_2 could not be removed out even by repeated heat treatment between room temperature and 600°C. The changes of laser-induced refractive index modulation Δn of the thermally-induced gratings were investigated as a function of the annealing times at 600°C. The Δn was estimated from the first order diffraction efficiencies. The Δn of the laser-induced grating before annealing was 6.9×10^{-4}, which was saturated after irradiation with 12 000 pulses. The Δn of the grating continuously increased after complete remove of the laser-induced grating by annealing up to 500°C. It saturated after annealing for 5 hours. The maximum Δn was 6.8×10^{-3}, which corresponds to a Δn value that is approximately ten times larger than that before annealing. The phase matching angle was not changed by this enhancement phenomenon, meaning that period of the grating was same. For conventional direct laser writing, a special photosensitizing process such as hydrogen loading is required to obtain such large Δn. Therefore, this enhancement phenomenon is useful for stabilization and for Δn enhancement.

4.2 Mechanism of thermally-induced refractive index changes

Figure 4(a) and 4(b) show scanning electron microscope images of the laser-induced gratings and the thermally-induced gratings after HF etching for 17 min. For this measurements, thermally-induced gratings were induced by annealing at 600°C for 80 min. Figure 4(a) presents that periodic surface relief can be observed. Reportedly, the etching rate of the SiO_2 surface increased after dense irradiation with vacuum ultraviolet light. For that reason, the formation of a relief structures in our samples is likely to be attributed to

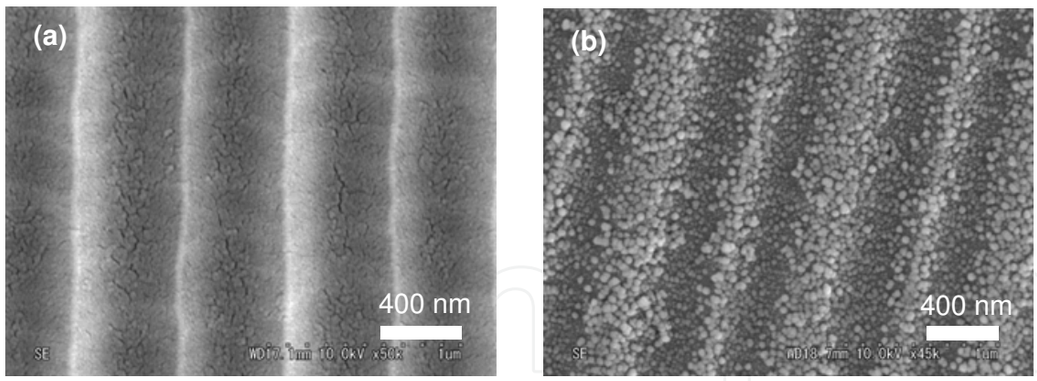

Fig. 4. Scanning electron microscope images of (a) a laser-induced grating and (b) a thermally-induced grating. Both samples were observed after HF etching. Reprinted with permission from Applied Physic Letters. Copyright 2004, American Institute of Physics.

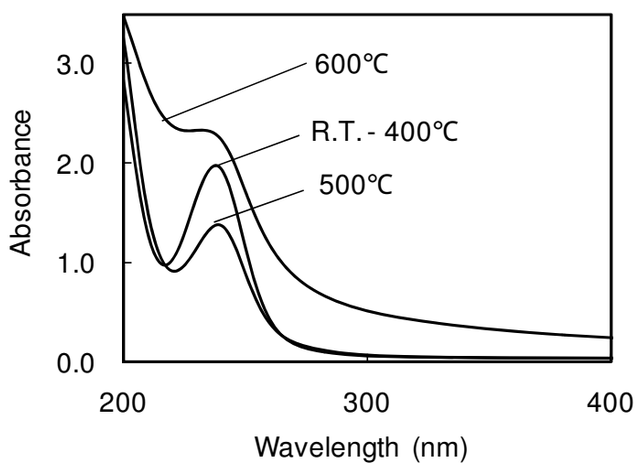

Fig. 5. Changes of absorption spectra of GeO_2-B_2O_3-SiO_2 thin films after annealing up to 600°C.

selective etching of the irradiated region. Figure 4(b) shows that nanoparticles of 20-40 nm diameters, which had higher resistance to HF solution than the glass matrix, were precipitated periodically on the thermally-induced grating surfaces. The pitch of the periodic structure was same as that of the laser-induced grating. From the XRD pattern of the glass film with the thermally-induced grating that was formed by annealing at 600°C for 80 min. Two signals at 2θ = 45.3 and 53.7 were detected. A slight diffraction peak at 2θ = 27.3 was also observable. These three signals in the pattern are assignable to the (220), (311) and (111) diffraction lines of cubic Ge crystal, respectively, which were never detected without nanoparticle precipitation.

Figure 5 shows the changes of absorption spectra of as-deposited GeO_2-B_2O_3-SiO_2 films before and after the annealing. The absorption band around 236 nm wavelength of the film before annealing is assignable to Ge related oxygen deficient defects such as neutral oxygen mono-vacancy or neutral oxygen di-vacancy related Ge ions. The absorption intensity due to the oxygen deficient defects did not change until 400°C, and then decreased at 500°C. However, marked increase of absorption was observed after the annealing at 600°C. Such changes were not observed for GeO_2-SiO_2 films. The spectral features after the annealing at 600°C were similar to those of glasses with Ge nanoparticles in previous report (Kawamura,

et al., 1996). As the diameter of the nanoparticels decreases, the absorption edge markedly shifts to shorter wavelength because of the size effect. The edge of the GeO_2-B_2O_3-SiO_2 films is located about 300 nm wavelength, and absorption shoulder spreads to visible wavelength region. Therefore, it is considered that the origin of the thermally-induced grating is the periodic precipitation of crystalline Ge nanoparticles. There have been many studies on space-selective precipitation of metal nanoparticles in glass using laser irradiation. In their reports, nanoparticles were always precipitated in the laser irradiated region because the thermal or photochemical reaction during laser irradiation promoted nucleation (Charles, *et al.*, 1968). However, the following experimental revealed that the Ge nanoparticles were precipitated predominantly in the unirradiated region of our samples.

Figure 6 shows a scanning electron microscope image of two-dimensional (2D) thermally-induced grating after the HF etching. The 2D gratings were formed in the same manner as that for the 1D gratings. At first, 2D laser-induced grating was written in the film. Then, the sample was rotated by 90 degree in its own plane midway through irradiation. The pulse number at each dimension was 12 000. Finally, the resulting 2D gratings were annealed at 600°C for 80 min to obtain the 2D thermally-induced gratings. Island structures, which consist of many nanoparticles, were can be observed. The pulse number at the

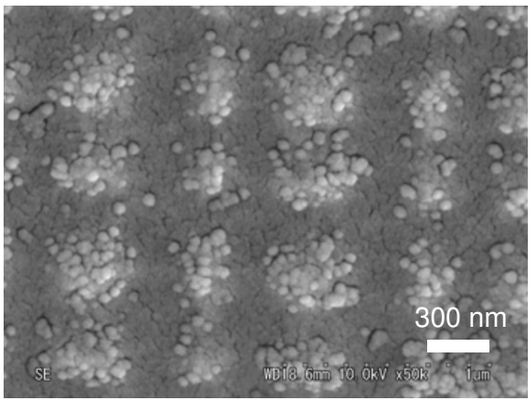

Fig. 6. Scanning electron microscope image of a 2D thermally-induced grating. The observation was carried out after HF wet etching. Reprinted with permission from Applied Physic Letters. Copyright 2004, American Institute of Physics.

crossover site of the 2D grating was twice as large as that at the noncrossover site. We confirmed that there was no marked difference in diffraction efficiencies of the laser-induced gratings and thermally-induced gratings by irradiation exceeding 12 000 pulses, meaning that the difference of the structural changes between the crossover and noncrossover sites are negligible. Therefore, the island-like precipitation in Figure 6 indicates that nanoparticles were precipitated predominantly in the unirradiated region.

We observed an etched surface of the unirradiated thin film after annealing at 600°C for 10 min. Although there were few nanoparticles, many dimples of approximately 300 nm diameters were observed on the surfaces. According to previous reports, the phase separation occurred in B_2O_3-SiO_2 glass below 600°C. Therefore, it is reasonable that the dimples represent the B_2O_3-rich phase, which is less stable against HF solution than other regions. It is notable that the phase separation occurred before the precipitation of Ge nanopartices. Assuming that the laser irradiation prior to annealing accelerated the phase separation that was induced by annealing at 600°C, the formation mechanism of thermally-

induced grating can be explained as follows. As a first step, the phase separation predominantly occurs in the laser irradiated region at the early stage of the annealing at 600°C. Formation of B_2O_3-rich phases increase Ge concentration in the surroundings. As a result, periodic distribution of chemical composition is induced in the grating region. In this case, Ge concentration in the irradiated region is lower than that in the unirradiated one. Therefore, the precipitation of Ge nanoparticles after sufficient annealing at 600°C might be suppressed in the irradiated region. Large refractive index modulation was likely to be induced by the precipitation of high refractive Ge nanoparticles. According to this model, the etch rate of the irradiated region will be higher than that in the unirradiated region because the irradiated region mainly consist of B_2O_3-rich phases. This prediction is consistent with the experimental result as shown in Figure 6.

5. Periodic structures consisting of nanoparticles in channel waveguides

Photonic band gap elements in channel waveguides have much higher potential for the integration with other functional components in single wafer. In this section, we present a periodic structures consisting of Ge nanoparticles, which have large PBG effect with high thermal stabilities, formed in the channel cores (Nishiyama, *et al.*, 2004).

5.1 Fabrication of periodic structures into channel waveguides

Figure 7 schematically shows the fabrication processes of the channel waveguides with thermally-induced gratings. At first, the grating structures with 530 nm pitch are written in GeO_2-B_2O_3-SiO_2 films with SiO_2 upper layers using KrF excimer laser with a phase mask. Annealing at 600°C for 20 min was carried out to induce the thermally-induced gratings. The Δn of the grating was 1.6 x 10^{-3} at 633 nm wavelength. The channel structures were subsequently fabricated using photolithography and plasma etching techniques. The width and height were of the core were 7.0 μm and 5.3 μm, respectively. Finally, the upper layers

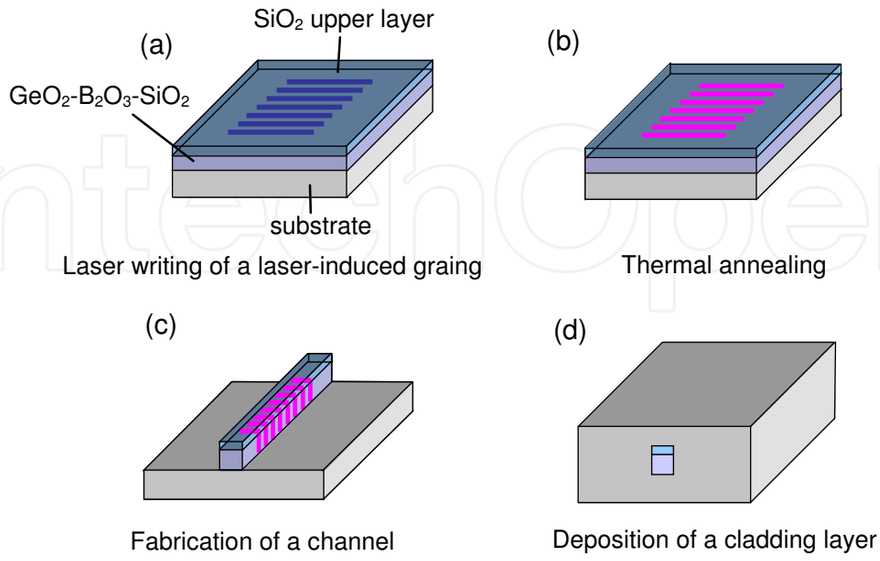

Fig. 7. Fabrication processes of channel waveguides with thermally-induced gratings.

of GeO_2-SiO_2 of 12 μm thickness were deposited to form single-mode waveguides. The interaction length of the grating was about 5 mm. Figure 8 shows the surfaces of as-fabricated channel cores, namely, before deposition of the cladding layer, after wet etching with 6% HF solution. For this observation, the SiO_2 upper layers were removed out by plasma etching process prior to the channel core fabrication. The channel core surfaces before HF etching in figure 8(a) were smooth in spite of the precipitation of nanoparticles. Especially, the sidewall roughness was also smooth. It is apparent that periodic relief patterns appeared on the channel surfaces after HF etching. The pitch of these periodic structures was 530 nm, which was identical to that of the laser-induced gratings written in the film before annealing. From Figure 8(d), the nanoparticles can be observed in the convex regions of the channels. In the section 5.2, we pointed out that the etch rate of the irradiated regions became higher than that of the unirradiated regions because of the predominant formation of B_2O_3-rich phases in the irradiated regions after annealing. In addition, Ge nanoparticles appeared mainly in the unirradiated regions. Therefore, these periodic relief structures are likely to be originated from the formation of thermally-induced gratings inside the channel. The periodic relief structures on the sidewall indicate that the Ge nanoparticles were precipitated not only near the film surfaces, but also across the films. The non-uniform relief patterns on the sidewall might result from the transmitted zero-order laser light, which was not completely suppressed by the phase mask during laser writing process.

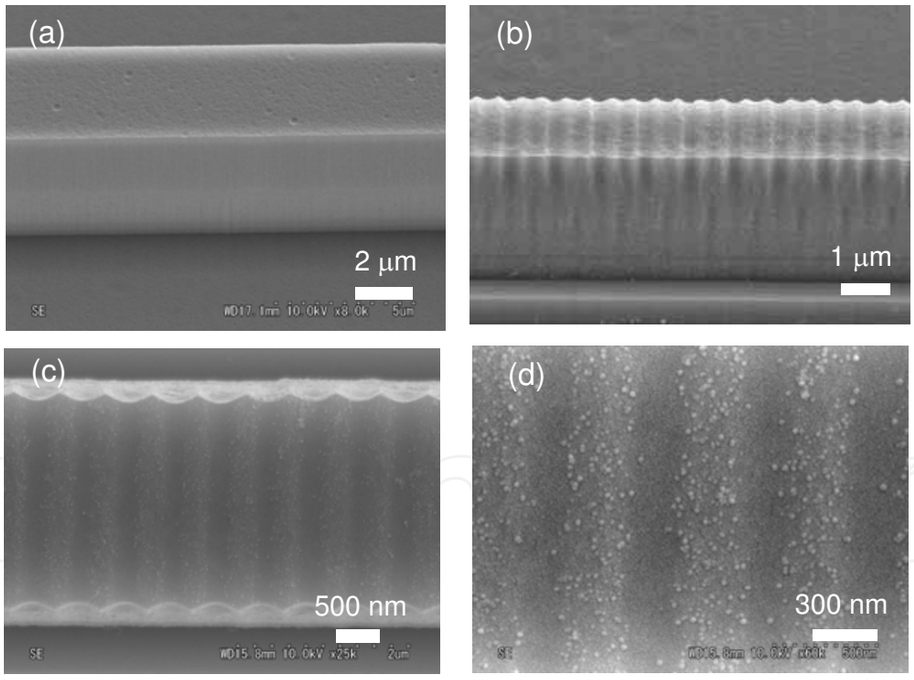

Fig. 8. Scanning electron microscope images of periodic structures consisting of nanoparticles (a) before and (b) after HF wet etching treatment, and images (c) from above and (d) of the enlarged one. Reprinted with permission from Optics Express. Copyright 2007, Optical Society of America.

Figure 9 shows transmission spectra for TE-like and TM-like modes when near-infrared wavelength light was coupled to the channel waveguides with the periodic structures

consisting of Ge nanoparticles. These optical properties were measured with an optical spectrum analyzer using a wavelength tunable laser diode as a light source. The incident beam was butt-coupled into channel waveguides using commercially available single-mode optical fibers. The depths and positions of the PBG were 37.77 dB at 1536.2 nm and 38.72 dB at 1537.6 nm, respectively, for TE-like and TM-like modes. Only one dip appeared for each polarization mode, indicating that the channel structures worked as a single-mode waveguide. Such strong PBG effects indicate that the refractive index modulation by periodic structures is large not only in the visible wavelength region, but also in the optical communication wavelength. The peak depths of both modes were similar, indicating that the Ge nanoparticles were uniformly precipitated in the unirradiated regions across the channel core, which is consistent with the relief formation on the sidewalls in Figure 8. The polarization dependence of the PBG wavelength is likely to be originated from the asymmetrical core structures. In this PBG device, the periodic structures were induced by annealing only for 20 min. In the section 5.1, the amount of Δn continuously increased with

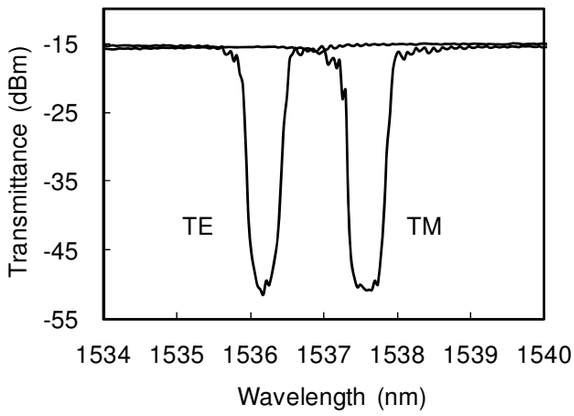

Fig. 9. Transmission spectra of PBG devices consisting of Ge nanoparticles in the channel.

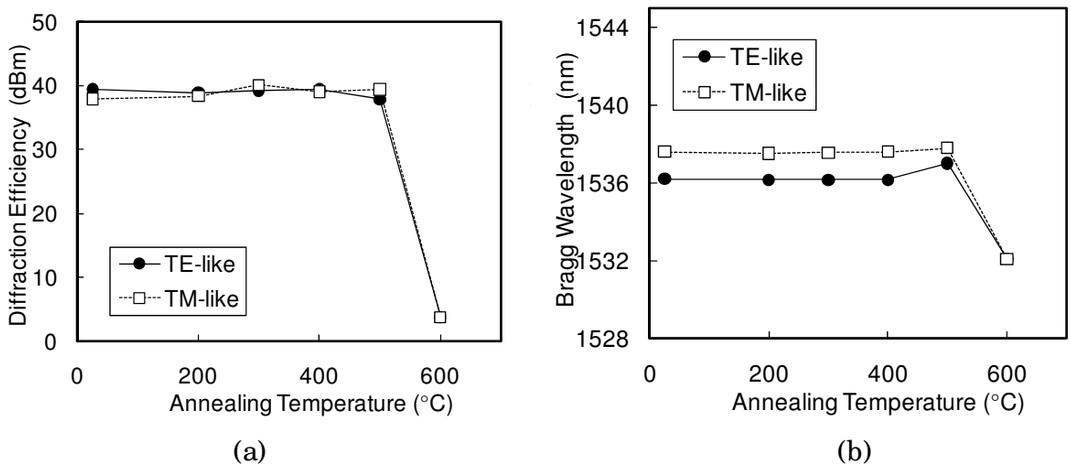

Fig. 10. (a) Diffraction efficiencies (PBG depths) and (b) Bragg wavelengths (PBG wavelengths) of thermally-induced gratings in channels.

annealing time at 600°C. Therefore, much stronger PBG effects are achievable after longer annealing time at the fabrication step (b) in Figure 7. Figure 10 (a) and 10(b) shows changes of the PBG depths and wavelength positions for both polarization modes after additional annealing from 200 to 600°C. The annealing time was 1 hour at each temperature. The conventional direct laser writing structures markedly decay even by annealing at 150°C. Compared to this, it is notable that the PBG depths for both modes exhibited no changes after annealing at 500°C. In particular, no changes of PBG depths and wavelengths were observed after annealing up to 400°C. The difference of the PBG wavelength between each polarization mode was changed from 1.4 nm to 0.8 nm without decay of PBG depths after annealing at 500°C. Such a decrease might be responsible for reduction of the residual thermal stress between the core and cladding layer of GeO_2-SiO_2 because the cladding layer was deposited at temperature lower than 500°C. These results indicate that the precipitation methods of Ge nanoparticles are effective to create much larger PBG effects with excellent thermal stabilities than those reported previously. The polarization dependence of the PBG wavelengths can be reduced between modes. Photonic band gap structures with higher efficiencies, thermal stability, and lower polarization dependence would be realized by optimization of fabrication conditions.

5.2 Direct laser writing of channel waveguides with periodic structures consisting of nanoparticle precipitation

In the last section, we presented the fabrication of PBG structures consisting of Ge nanoparticles in channel cores using photolithography and plasma etching processes. The devices exhibited strong PBG effects with high thermal stabilities. However, complicated vacuum processes and clean room environments are required. In this section, we present a fabrication process of PBG devices, which consist of Ge nanoparticles, inside channel waveguides only using direct laser writing and subsequent thermal annealing.

Figure 11 shows changes of refractive indices at 633 nm wavelength of the unirradiated GeO_2-B_2O_3-SiO_2 film and homogeneously irradiated film against an annealing time at 600°C. The laser fluence and pulse number for preparation of the irradiated film were 180 mJ cm^2/ pulse and pulse number of 27 000. By irradiation, refractive index increased by 3.1 x 10^{-3}. Annealing for 10 min markedly decreased this difference of refractive index between both films to 0.5 x 10^{-3}. Refractive indices of both films increased after annealing time longer than 10 min because of the precipitation of Ge nanoparticles with higher refractive indices than those of glass matrix. It is notable that the rate of the refractive index increase for the irradiated film was much lower than that for the unirradiated one. Due to this difference of increase rate, the refractive index of the unirradiated film became higher than that of the irradiated one after annealing after 10 min. Such thermally-induced refractive index difference exhibited high stabilities against repeated annealing up to 500°C.

Based on this unique behavior of refractive index of the GeO_2-B_2O_3-SiO_2 films of 4 μm thickness, we fabricate the PBG devices inside channel cores. Figure 12 shows the fabrication processes of the PBG devices and the expected refractive index distribution at each process. First, grating structures were written in a GeO_2-B_2O_3-SiO_2 film using KrF excimer laser through a phase mask. Then, the irradiation through a Cr mask with a straight line pattern of 7 μm width on a SiO_2 substrate was performed under the condition of the laser fluence of

180 mJ/ cm²/ pulse and pulse number of 27 000. Finally, the samples were annealed at 600°C for 20 min. The refractive index distribution was inverted after this annealing step, resulting PBG devices in channel cores. Propagation loss of the waveguides increased with the annealing time at 600°C. The loss before and after the annealing for 1 hour was 0.4 and 1.4 dB/ cm at 1545 nm wavelength, respectively.

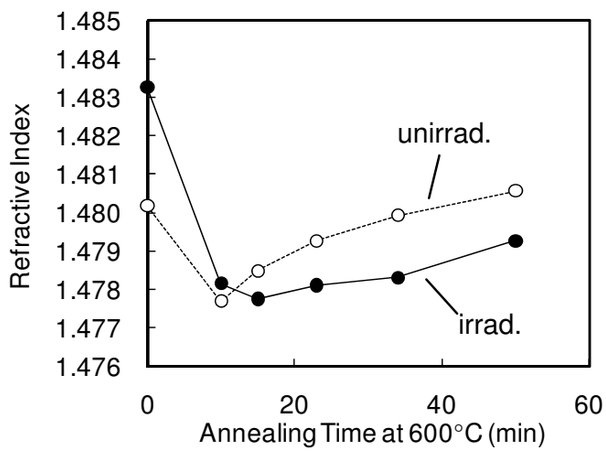

Fig. 11. Changes of refractive indices of unirradiated and irradiated films.

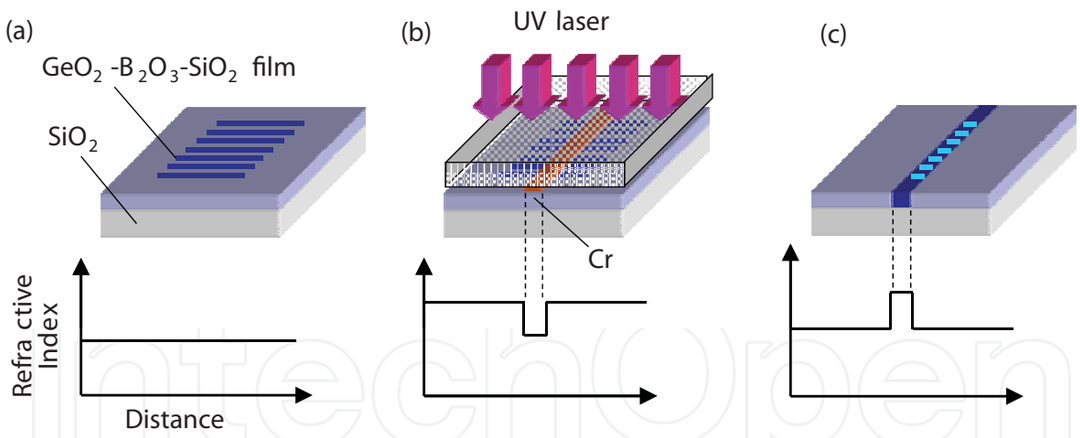

Fig. 12. Fabrication processes for the periodic structures consisting of Ge nanoparticles in channels. (a) Laser writing of the gratings, (b) laser irradiation through a Cr mask, and (c) thermal annealing at 600ºC for 20 min

An optical microscope image of the waveguide structures is shown in Figure 13(a). We can see that a brown slight line was induced in the film. The line width was approximately 6 μm, which was consistent with the width of the Cr mask line. In the GeO_2-B_2O_3-SiO_2 film used in this study, intense absorption bands are induced in ultraviolet-visible wavelength regions by annealing at 600°C, which is responsible for the precipitation of Ge nanoparticles. The laser irradiation suppresses the nanoparticle precipitation. Therefore, we can consider that the nanoparticle concentration of the straight line area became higher than that of the

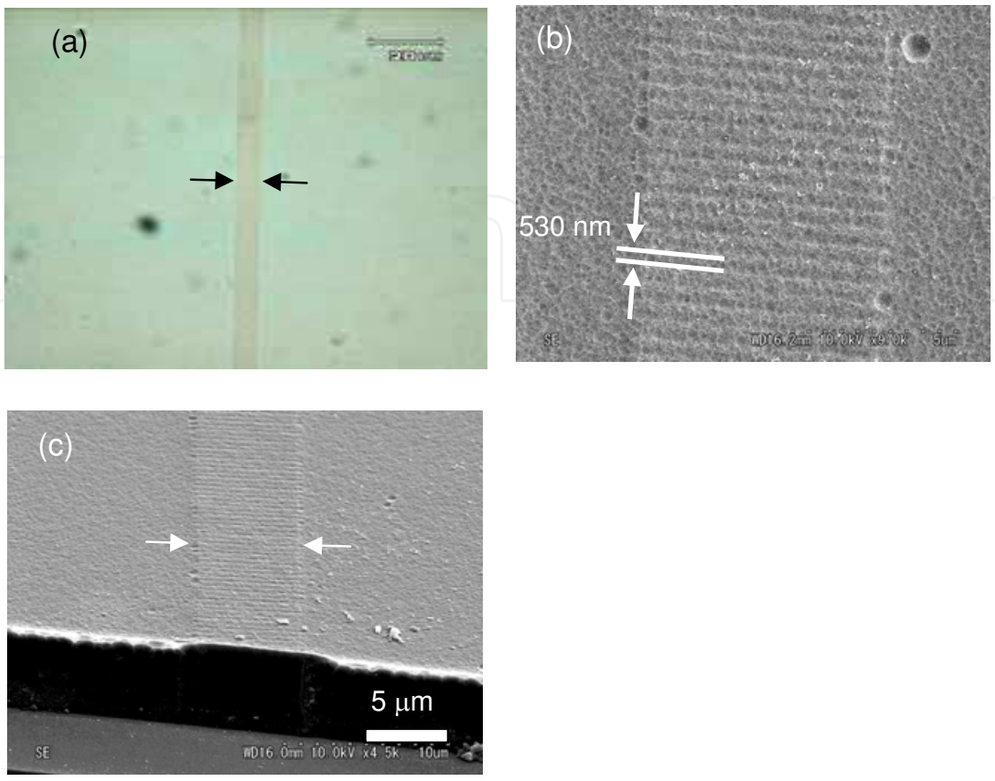

Fig. 13. (a) Optical microscope image of a channel core region and scanning electron microscope images of (b) top-view and (c) overall view of a PBG devices consisting of nanoparticles. Reprinted with permission from Journal of Physics. Copyright 2009, IOP publishing.

surroundings, and that brown-colored straight line is originated from the absorption shoulder of the nanoparticles. Figure 13(b) and (c) shows scanning electron microscope images of top view an overall view of the films after HF etching. Although it was difficult to recognize individual nanoparticle by this observation because the annealing time was as short as 20 min, the periodic structure and the channel core were observable in the film. No surface reliefs were detected before the HF etching because of their smooth surfaces. The channel width and period of the structures were 7 μm and 530 nm, respectively, which were identical with those of the photoimprinted patterns in Figure 12(b). Bright lines in the periodic structures are likely to be aligned aggregated nanoparticles. Note that the periodic structures at clad areas (outside areas of the cores in the film) were not visible. This erase is most likely due to irradiation with higher fluence in Figure 12(b) than that in Figure 12(a). By this irradiation, laser-induced refractive index contrast in Figure 12(b) decayed because larger refractive index changes can be induced by higher fluence. This confinement of the periodic structures in the core can avoid coupling of propagation light to clad and leaky modes. From Figure 11, the refractive index difference between core and cladding regions for the in-plane direction was approximately 1.2×10^{-3} at 633 nm wavelength. This periodic

structures exhibited peaks of 18.0 dB at 1532.7 nm and 18.7 dB at 1533.1 nm for the TE-like mode and TM-like mode, respectively, in transmission spectra. These peaks indicate that the periodic structures worked as PBG devices inside the channels.These PBG devices exhibited high thermal stabilities compared to the conventional laser-induced PBG ones. The structural changes of the laser-induced gratings were almost completely erased after repeated annealing at 400°C. In contrast, it is notable that no remarkable changes of PBG depths and wavelengths were observed for the periodic structures consisting of Ge nanoparticles even after heat treatment at 500°C.

6. Summary

In this chapter, we presented the fundamentals of pulse laser-induced structural changes of SiO_2-based glasses and demonstrated the fabrication of PBG devices consisting of crystalline Ge nanoparticles using a combined process of direct laser writing and subsequent thermal annealing. Large refractive index modulations with high thermal stabilities were induced by this combined process. The periodic structures in channel cores exhibited intense PBG effects of nearly 40 dB for both polarization modes. And no changes of the PBG effects were observed even after repeated heat treatment up to 500°C. Optimization of pulse laser irradiation and phase change conditions can realize devices with much larger PBG effects using direct laser writing techniques.

7. References

Åslund, M. & Canning, J. (2000). Annealing properties of gratings written into UV-presensitized hydrogen-outdiffused optical fiber, *Optics Letters*, Vol. 25, 692-694.

Baker, S. R.; Rourke, H. N.; Baker, V. & Goodchild (1997). Thermal decay of fiber Bragg gratings written in boron and germanium codoped silica fiber, *Journal of Lightwave Technology*, Vol.15, 1470-1477.

Borrelli, N. F.; Allan, D. C. & Modavis, R. A. (1999). Direct measurement of 248- and 193-nm excimer-induced densification in silica-germania waveguide blanks, *Journal of Optical Society of America B*, Vol. 16, 1672-1679.

Charles, R. J. & Wagstaff, F. E. (1968). Metastable Immiscibility in the B_2O_3-SiO_2 System. *Journal of the American Ceramics Society*, Vol. 51, 16-20.

Cordier P.; Doukhan, J. C.; Fertein, E.; Bernage, P.; Niay, P.; Bayon, J. F. & Georges, T. (1994). TEM observation of structural changes in glass associated to Bragg grating inscription in a germanosilicate optical fiber preform, *Optics Communications*, Vol. 111, 269-275.

Cordier, P.; Dupont, S.; Douay, M.; Martinelli, G.; Bernage, P.; Niay, P.; Bayon, J. F. & Dong, L. (1997). Evidence by transmission electron microscopy of densification associated to Bragg grating photoimprinting in germanosilicate optical fibers, *Applied Physics Letters*, Vol. 70, 1204-1206.

Dong, L.; Archambault, J. L.; Reekie, L.; Russel, P. St. J. & Payne, D. N. (1995). Photoinduced absorption change in germanosilicate performs: evidence for the color-center model of photosensitivity, *Applied Optics*, Vol. 34, 3436-3440.

Douay, M.; Xie, W. X.; Taunay, T.; Bernage, P.; Niay, P.; Cordier, P.; Poumellec, B.; Dong, L.; Bayon, J. F.; Poignant, H. & Delevaque, R. (1997). Densification Involved in the UV-Based Photosensitivity of Silica Glasses and Optical Fibers, *Journal of Lightwave Technology*, Vol. 15, 1329-1342.

Erdogan, T.; Mizrahi, V.; Lemaire, P. J. & Monroe, D. (1994). Decay of ultraviolet-induced fiber Bragg gratings, *Juranl of Applied Physics*, Vol. 76, 73-80.

Fonjallaz, P. Y.; Limberger, H. G. & Salathé, R. P. (1995). Tension increase correlated to refractive-index change in fibers containing UV-written Bragg gratings, *Optics Letters*, Vol. 20, 1346-1348.

Hand, D. P.; & Russell, P. St. J. (1990). Photoinduced refractive-index changes in germano-silicate fibers, *Optics Letters*, Vol.15, 102-104.

Hill, K. O. & Meltz, G. (1997). Fiber Bragg grating technology fundamentals and overview, *Journal of Lightwave Technology*, Vol. 15, 1263-1276.

Kawamura, K.; Hosono, H. & Kawazoe, H. (1996). Proton-implantation-induced nanosized Ge crystal formation in SiO_2:GeO_2 glasses. *Journal of Applied Physics*, Vol. 80, 1357-1363.

Kim, B. H.; Park, Y., Ahn, T. J; Kim, D. Y.; Lee, B. H.; Chung, Y.; Peak, U. C. & Han, W. T. (2001). Residual stress relaxation in the core of optical fiber by CO_2 laser irradiation, *Optics Letters*, Vol. 26,1657-1659.

Kherbouche, F. & Poumellec, B. (2001). UV-induced stress field during Bragg grating inscription in optical fibers, *Journal of Optics: Pure and Applied optics*, Vol. 3, 429-439.Ky, N. H.; Limberger, H. G.; Salathé, R. P.; Cochet, F. & Dong, L. (2003). UV-irradiation induced stress and index changes during the growth of type-I and type-II fiber gratings, *Optics Communications*, Vol. 225, 313-318.

Miura, K.; Qiu, J; Inouye, H.; Mitsuyu, T. & Hirao, K. (1997). Photowritten optical waveguides in various glasses with ultrashort pulse laser, *Applied Physics Letters*, Vol. 71, 3329-3331.

Nishii, J; Kitaka, K.; Nishiyama, H. & Miyamoto, I. (2002). Thermally stabilized photoinduced Bragg gratings, *Applied Physics Letters*, Vol. 81, 2364-2366.

Nishiyama, H.; Kitaka, K.; Nishii, J. & Miyamoto, I. (2003). Thermo- and photosensitive GeO_2-B_2O_3-SiO_2 thin glass films, *Japanese Journal Applied Physics*, Vol. 42, 559-563.

Nishiyama, H.; Miyamoto, I.; Matsumoto, S.; Saito, M.; Kintaka, K. & Nishii, J. (2004). Direct laser writing of thermally stabilized channel waveguides with Bragg gratings, *Optics Express*, Vol. 12, 4589-4595.

Nishiyama, H.; Miyamoto, I.; Matsumoto, S.; Saito, M.; Fukumi, K.; Kintaka, K. & Nishii, J. (2004). Periodic precipitation of crystalline Ge nanoparticles in Ge-B-SiO_2 thin glass films, *Applied Physics Letters*, Vol 85, 3734-3736.

Nishiyama, H.; Miyamoto, I.; Hirata, Y. & Nishii, J. (2007). Periodic structures consisting of germanium nanoparticles in buried channel waveguides, *Optics Express*, Vol. 15, 2047-2054.

Nishiyama, H.; Nishii, J. & Hirata, Y. (2009). Periodic structures in GeO_2-B_2O_3-SiO_2 glass films fabricated using ultraviolet laser pulses, Journal of Physics: Conference Series, Vol. 165, 012049-1-4.

Poumellec, B.; Niay, P.; Douay, M. & Bayon, J. F. (1996). The UV-induced refractive index grating in Ge:SiO_2 preforms: additional CW experiments and the macroscopic origin of the change in index, *Journal of Physics D: Applied Physics*, Vol. 29, 1842-1853.

Poumellec, B.; Guènot, P.; Riant, I.; Sansonetti, P.; Niay, P.; Bernage, P. & Bayon, J. F. (1995). UV induced densification during Bragg grating inscription in Ge:SiO_2 preforms, *Optical Materials*, Vol. 4, 441-449.

Svalgraad, M.; Poulsen, C. V.; Bjarklev, A. & Poulsen, O. (1994). Direct UV writing of buried single mode channel waveguides in Ge-doped silica film, *Electronics Letters*, Vol. 30, 1401-1403.

Laser Pulse Phenomena and Applications
Edited by Dr. F. J. Duarte

ISBN 978-953-307-405-4
Hard cover, 474 pages
Publisher InTech
Published online 30, November, 2010
Published in print edition November, 2010

Pulsed lasers are available in the gas, liquid, and the solid state. These lasers are also enormously versatile in their output characteristics yielding emission from very large energy pulses to very high peak-power pulses. Pulsed lasers are equally versatile in their spectral characteristics. This volume includes an impressive array of current research on pulsed laser phenomena and applications. *Laser Pulse Phenomena and Applications* covers a wide range of topics from laser powered orbital launchers, and laser rocket engines, to laser-matter interactions, detector and sensor laser technology, laser ablation, and biological applications.

How to reference
In order to correctly reference this scholarly work, feel free to copy and paste the following:

Hiroaki Nishiyama and Junji Nishii (2010). Photoinduced Structural Changes of Doped SiO_2 Glasses using Ultraviolet Laser Pulses, Laser Pulse Phenomena and Applications, Dr. F. J. Duarte (Ed.), ISBN: 978-953-307-405-4, InTech, Available from: http://www.intechopen.com/books/laser-pulse-phenomena-and-applications/photoinduced-structural-changes-of-doped-sio2-glasses-using-ultraviolet-laser-pulses

INTECH
open science | open minds

InTech Europe
University Campus STeP Ri
Slavka Krautzeka 83/A
51000 Rijeka, Croatia
Phone: +385 (51) 770 447
Fax: +385 (51) 686 166
www.intechopen.com

InTech China
Unit 405, Office Block, Hotel Equatorial Shanghai
No.65, Yan An Road (West), Shanghai, 200040, China
中国上海市延安西路65号上海国际贵都大饭店办公楼405单元
Phone: +86-21-62489820
Fax: +86-21-62489821

IntechOpen